Selective Assist Strategy by Using Lightweight Carbon Frame Exoskeleton Robot

Jun-ichiro Furukawa, *Member, IEEE*, Shotaro Okajima, *Member, IEEE*, Qi An, *Member, IEEE*, Yuichi Nakamura, and Jun Morimoto, *Member, IEEE*

***Abstract*—Exoskeleton robots need to always actively assist the user's movements otherwise robot just becomes a heavy load for the user. However, estimating diversified movement intentions in a user's daily life is not easy and no algorithm so far has achieved that level of estimation. In this study, we rather focus on estimating and assisting a limited number of selected movements by using an EMG-based movement classification and a newly developed lightweight exoskeleton robot. Our lightweight knee exoskeleton is composed of a carbon fiber frame and highly backdrivable joint driven by a pneumatic artificial muscle. Thus, our robot does not interfere with the user's motions even when the actuator is not activated. As the classification method, we adopted a positive-unlabeled (PU) classifier. Since precisely labeling all the selected data from large-scale daily movements is not practical, we assumed that only part of the selected data was labeled and used a PU classifier that can handle the unlabeled data. To validate our approach, we conducted experiments with five healthy subjects to selectively assist sit-to-stand movements from four possible daily motions. We compared our approach with two classification methods that assume fully labeled data. The results showed that all subject's movements were properly assisted.**

***Index Terms*—Prosthetics and exoskeletons, intention recognition, optimization and optimal control.**

Manuscript received September 9, 2021; accepted January 17, 2022. Date of publication February 7, 2022; date of current version February 16, 2022. This letter was recommended for publication by Associate Editor J.-J. Cabibihan and Editor P. Valdastri upon evaluation of the reviewers' comments. This work was supported in part by RIKEN-Kyushu University of Science and Technology Hub Collaborative Research Program and in part by JSPS KAKENHI under Grants JP21K17836 and JP21H04894. *(Corresponding author: Jun-ichiro Furukawa.)*

Jun-ichiro Furukawa is with the Man-Machine Collaboration Research Team, Guardian Robot Project, RIKEN, Kyoto 619-0288, Japan, and also with the Department of Brain Robot Interface, ATR Computational Neuroscience Labs, Kyoto 619-0288, Japan (e-mail: junichiro.furukawa@riken.jp).

Shotaro Okajima is with the CBS-TOYOTA Collaboration Center Intelligent Behavior Control Unit, RIKEN, Nagoya 463-0003, Japan (e-mail: shotaro.okajima@riken.jp).

Qi An is with the Faculty of Information Science and Electrical Engineering, Kyushu University, Fukuoka 8190395, Japan (e-mail: anqi@ait.kyushu-u.ac.jp).

Yuichi Nakamura is with the Man-Machine Collaboration Research Team, Guardian Robot Project, RIKEN, Kyoto 619-0288, Japan, and also with the Academic Center for Computing and Media Studies, Kyoto University, Kyoto 6068501, Japan (e-mail: yuichi@media.kyoto-u.ac.jp).

Jun Morimoto is with the Man-Machine Collaboration Research Team, Guardian Robot Project, RIKEN, Kyoto 619-0288, Japan, with the Department of Brain Robot Interface, ATR Computational Neuroscience Labs, Kyoto 619-0288, Japan, and also with the Graduate School of Informatics, Kyoto University, Kyoto 6068501, Japan (e-mail: xmorimo@atr.jp).

This letter has supplementary downloadable material available at https://doi.org/10.1109/LRA.2022.3148799, provided by the authors.

Digital Object Identifier 10.1109/LRA.2022.3148799

I. Introduction

AGING society accelerating in recent years calls for new assistive devices that support daily activities such as walking and standing-up motion using robotics technologies, and lower limb exoskeleton robots have been studied to meet the demand [1]–[3].

Such an exoskeleton robot needs to always actively assist the user's movement otherwise robot just becomes a heavy load for the user. Although the hardware is getting lighter [4], assistance based on the estimated user's movement intention is often provided only in a limited range of behavior [5].

Thanks to recent progress in wearable sensor technologies, measuring a wide variety of motions are becoming possible [6]. However, estimating various movement intentions in a user's daily life is not easy because many confusing motions can be contained in the large-scale daily movement, and precisely labeling all the selected data is not practical. Therefore, no assist algorithm so far has achieved that level of movement estimation.

In this study, we focus on estimating and assisting a limited number of movements in a realistic situation by using electromyography (EMG) based movement classification method and a newly developed lightweight exoskeleton robot. Our lightweight knee exoskeleton robot is composed of a carbon fiber frame and highly backdrivable joint driven by pneumatic artificial muscles (PAM) (Fig. 1(a)). Thus, our robot does not interfere with the user's motions even when the actuator is not activated. In our approach, we select an assistive control policy based on the estimated user's motion intentions (Fig. 1(b)). To estimate the motion intention, we adopted a positive and unlabeled learning framework [7] assuming that only part of the selected data was labeled. Through our experiment with five healthy subjects, we evaluated our approach with two baseline methods. As the target movements to be assisted, in our evaluations, we focused on the sit-to-stand (STS) motion among four candidate daily motions. The contributions of our study are following:

1) We newly developed a lightweight knee exoskeleton robot. The robot is composed of a carbon fiber frame and highly backdrivable joint driven by a pneumatic artificial muscle (PAM).
2) We propose the selective assist strategy in which the lightweight exoskeleton robot only assists a limited number of movements among a variety of possible daily motions. For detecting a target movement, we adopted a positive-unlabeled (PU) classifier.

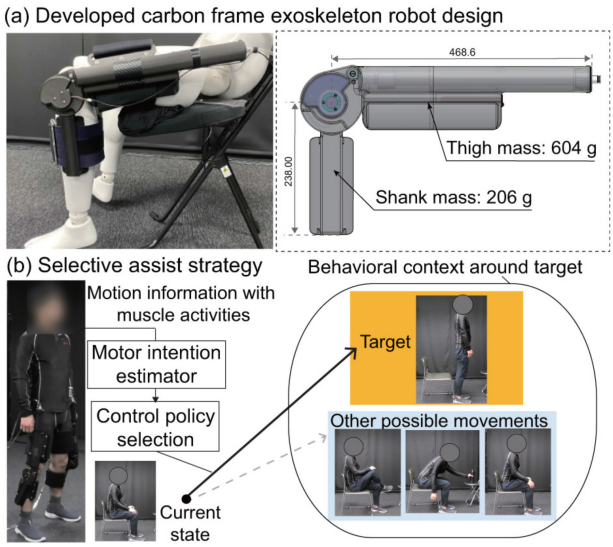

Fig. 1. Exoskeleton Robot and our control approach. (a) Developed carbon frame exoskeleton robot. (b) Proposed selective assist strategy. In our approach, assistive policy is selected among candidate daily motions by using an EMG-based movement classification method constructed in a positive-unlabeled (PU)-learning framework and assists user's motion with a newly developed lightweight exoskeleton robot.

3) We evaluated our proposed method in a selective assist task for the sit-to-stand movement. We also empirically showed how users were improperly assisted if the user's movement intention was incorrectly estimated. Furthermore, we evaluated how our robot does not interfere with the user's non-target motions.

The rest of this article is organized as follows. Section II describes related works. In Section III we introduce our newly developed lightweight exoskeleton robot and estimation approach of user's intention. Section IV describes our experimental setups. Section V shows our experimental results. Finally, the conclusion is provided in Section VI.

II. Related Works

To assist the user with the exoskeleton robot, pre-designed policies, such as guiding the user in a predefined trajectory [8] were often used to control and trigger-based interventions are natural if the user only performs the expected motion [9].

In these approaches, triggers from joint angles are commonly used as the user's motion intention [10]. In this method, the robot sensitively responds to the trigger and if the user unintentionally performs other motions, the assistive motion generated by the pre-designed policies may not be appropriate. Another candidate approach to set the trigger is using EMG. For example, estimating user's movement intention by classification method [11] such as support vector machine (SVM) [12], [13] or linear discriminant analysis (LDA) [14], [15]. The classification results were used to select pre-designed control output associated with the motion labels. Since the EMG contains the useful user's motion intentions, it can trigger more diversely than angle-only monitoring. However, since this approach assumes the generation of pre-designed control output within a fully labeled motion context, these traditional classification methods are unsuitable

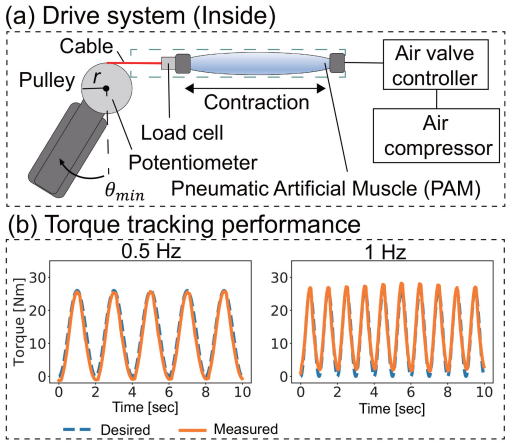

Fig. 2. Exoskeleton Robot: (a) joint torque driving system by pneumatic artificial muscle (PAM) with an effective length of 324 mm and an inner diameter of 20 mm. PAM is provided by FESTO-ϕ 20. Air valve is provided by NORGREN-VP5010SBJ111H00. Maximum allowable torque is 52 Nm for one knee joint. (b) Torque tracking performance. Root mean square error of 0.5 Hz is 1.86 Nm, and that of 1 Hz is 1.58 Nm.

for selecting control policy in practical situations where precise labeling of all data is not easy and unclear behaviors occur.

In this study, we introduce our selective assist strategy based on the estimated user's intention from the classifier which is composed in the positive and unlabeled (PU)-learning framework [7], and evaluate the approach with our newly developed lightweight exoskeleton robot in the situation assuming that the user's behavior other than the target motion (STS) can occur. Through the assistive experiments with five healthy subjects, we evaluate the difference between the proposed approach and the conventional standard approaches. To the best of our knowledge, this paper also describes the results of the first examine how the exoskeleton robot behaves when the user performs an unlabeled action.

III. Methods

This section first introduces our newly developed lightweight exoskeleton robot. Then, an estimation approach of the user's motor intention to drive the exoskeleton robot is shown.

A. Lightweight Knee Exoskeleton Robot

Fig. 1(a) shows our newly developed exoskeleton robot focused on assisting the knee joint, which requires a large amount of torque. This robot is attached by fixing it to each thigh and leg with a band. The skeleton is made of carbon resin material, so it is strong and lightweight: one leg is about 810 g without including an air compressor, battery, and control PC. Fig. 2(a) shows the driving system and it is composed of a highly backdrivable joint driven by Pneumatic Artificial Muscle (PAM) which is placed inside a tubular carbon skeleton.

The desired joint torque is generated by the PAM as follows:

$$\tau_{pam} = rF_{pam} \tag{1}$$

where r is the pulley radius and F_{pam} is the PAM force generated by the path contraction of the spiral fibers embedded in a pneumatic bladder. We use the PAM provided by FESTO [16]

and the relationship between the force and contraction rate of the PAM can be written by 2nd order polynomial. On the other hand, there is a linear relationship between pressure increase and force generation at the same contraction rate. From these characteristics, the quadratic model of PAM force can be written as:

$$F_{pam} = \frac{(f_u - f_l)P + P_u f_l - P_l f_u}{P_u - P_l} \tag{2}$$

where P is the inner pressure of PAM. P_u and P_l are constant pressure 0.8 MPa and 0.7 MPa. f_u is a quadratic force model when pressure is set to 0.8 MPa and f_l is a quadratic force model when pressure is set to 0.7 MPa:

$$\begin{aligned} f_u &= a_u\alpha^2 + b_u\alpha + c_u \\ f_l &= a_l\alpha^2 + b_l\alpha + c_l, \end{aligned}$$

where α is the contraction rate of the PAM. The contraction rate is calculated by the joint angle θ and minimum joint angle θ_{min}: $\alpha = \frac{r(\theta - \theta_{min})}{l_{pam}}$, where l_{pam} is the effective length of the PAM. Each parameter a_u, b_u, c_u, a_l, b_l and c_l is calculated by the calibration using the contraction rate and load cell. The details of the pressure-force model and calibration process were introduced in our previous studies [17]–[19]. From equations (1) and (2), the exoskeleton robot is pneumatically driven when the desired joint torque is applied. Fig. 2(b) shows the torque tracking performance of the exoskeleton robot. We obtained the data by generating desired torque with a range from 0 to 26 Nm with 0.5 and 1 Hz. Root mean square errors are 1.86 and 1.58 Nm, respectively.

B. Control Method Based on User's Intention

Fig. 3(a) shows the overview of our control approach. In this subsection, we first introduce an approach to find standing-up motion intention based on the classification in a PU-learning framework and then show the control policy deriving method.

1) Find Standing-Up Motion Intention Based on Classification: To find the user's intention for standing-up motion from obtained sensor signals, we introduce a framework to learn a classifier from positive and unlabeled data (PU-learning) [20].

In the traditional classification, learning algorithms work in a supervised setting, where the training data is assumed to be fully labeled, e.g., training example is a tuple $(\mathbf{z}, y)$, where $\mathbf{z}$ is the vector of attribute values and y is class value, and a classifier is trained to be able to distinguish between two classes: "positive" if $y = 1$ and "negative" if $y = 0$ of instances based on their attributes. On the other hand, a classifier of the PU-learning is trained in a different setting where only some of the positive examples in the training data are labeled and the negative examples are unlabeled. A PU-data-set is represented as a set of triples $(\mathbf{z}, y, s)$ with additional variable s (let $s = 1$ if the example $\mathbf{z}$ is labeled, and let $s = 0$ if $\mathbf{z}$ is unlabeled). The class y is not observed, but information about it can be derived from the value of s: if the example is labeled $s = 1$, then it belongs to the positive class, and if $s = 0$, it belongs to either class. The goal of PU-learning in this situation is to represent

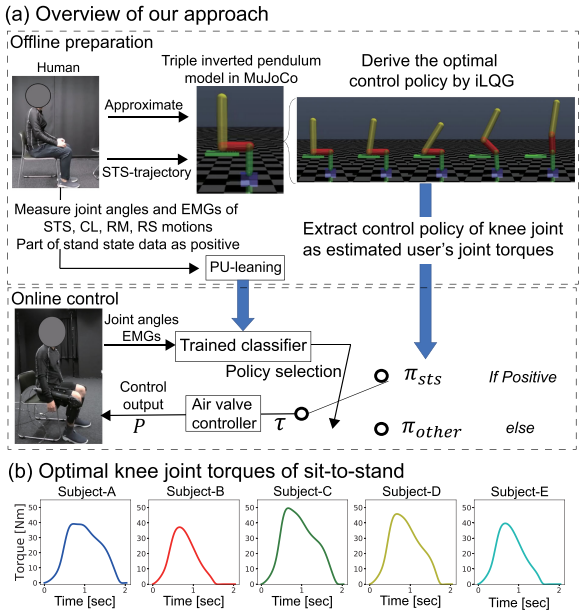

Fig. 3. (a) Overview of our approach. Control policy is selected by EMG-based movement classifier constructed from PU-learning. Control policy to assist STS motion π_{sts} is derived by using iLQG with physics simulator MuJoCo in which built a human model. π_{other} is gravity compensation term to cancel out weight of thigh robot unit when user's legs are in contact with ground. (b) Optimal knee joint torques derived from iLQG.

a function $f(\mathbf{z})$ with a probability from positive and unlabeled data-set such that: $f(\mathbf{z}) = p(y = 1|\mathbf{z})$.

To implement the PU-learning framework in this study, we adopt a basic algorithm [7]. The PU-learning starts with the fact that only positive examples are labeled:

$$p(s = 1|\mathbf{z}, y = 0) = 0, \tag{3}$$

and with the assumption that positive labeled examples are "selected completely at random" (SCAR) independent from their attributes:

$$c = p(s = 1|\mathbf{z}, y = 1) = p(s = 1|y = 1). \tag{4}$$

Then, considering $p(s = 1|\mathbf{z})$ together with the equations (3) and (4), and applying Bayes' rule, the following relationship is derived.

$$\begin{aligned} p(s = 1|\mathbf{z}) &= p(y = 1 \wedge s = 1|\mathbf{z}) \\ &= p(y = 1|\mathbf{z})p(s = 1|y = 1) \end{aligned} \tag{5}$$

From the clear relational expression $p(y = 1|\mathbf{z}, s = 1) = 1$ and the equation (5), the following relationship is also derived:

$$\begin{aligned} p(y = 1|\mathbf{z}, s = 0) &= \frac{p(s = 0|\mathbf{z}, y = 1)p(y = 1|\mathbf{z})}{p(s = 0|\mathbf{z})} \\ &= \frac{[1 - p(s = 1|\mathbf{z}, y = 1)]p(y = 1|\mathbf{z})}{1 - p(s = 1|\mathbf{z})} \\ &= \frac{1 - c}{c}\frac{p(s = 1|\mathbf{z})}{1 - p(s = 1|\mathbf{z})} \doteq \omega(\mathbf{z}). \end{aligned} \tag{6}$$

Here, let the goal be to estimate the expected value $E_{p(\mathbf{z},y,s)}[h(\mathbf{z}, y)]$ for any function h, where $p(\mathbf{z}, y, s)$ is the

overall distribution. We concisely write it as $E[h]$, which is calculated by definition as follows:

$$\begin{aligned} E[h] &= \int_{\mathbf{z},y,s} h(\mathbf{z},y)p(\mathbf{z},y,s) \\ &= \int_{\mathbf{z}} p(\mathbf{z}) \sum_{s=0}^{1} p(s|\mathbf{z}) \sum_{y=0}^{1} p(y|\mathbf{z},s)h(\mathbf{z},y) \\ &= \frac{\sum_{\mathbf{z},s=1} h(\mathbf{z},1)}{m} \\ &\quad + \frac{\sum_{\mathbf{z},s=0} \omega(\mathbf{z})h(\mathbf{z},1) + (1-\omega(\mathbf{z}))h(\mathbf{z},0)}{m}, \end{aligned} \tag{7}$$

where m is the cardinality of the training data-set. From this equation (7), positive data are given unit weight and unlabeled data are duplicated; one copy of each unlabeled example is made positive with weight $\omega(\mathbf{z})$ and the other copy is made negative with weight $1-\omega(\mathbf{z})$, and then, learn the classifier with this weighting samples. Here, considering $h(\mathbf{z},y) = y$, we obtain

$$\begin{aligned} E[y] &= p(y=1) \\ &= \frac{\sum_{\mathbf{z},s=1} 1}{m} + \frac{\sum_{\mathbf{z},s=0} \omega(\mathbf{z})1 + (1-\omega(\mathbf{z}))0}{m} \\ &= \frac{1}{m}\left(n + \sum_{\mathbf{z},s=0} \omega(\mathbf{z})\right), \end{aligned} \tag{8}$$

where n is the cardinality of the labeled training data-set and this estimator is greater than n/m. By the above PU-learning, we create a classifier that estimates the intention of standing-up motion from positive and unlabeled behavioral data.

2) Control Policy Allocation: In our assistive strategy, we switch a control policy based on the output of the classifier so that appropriate policy is selected according to the user's intention:

$$\pi^* \leftarrow \begin{cases} \pi_{sts} & \text{if} \quad y = 1 \\ \pi_{other} & \text{if} \quad y \neq 1, \end{cases} \tag{9}$$

where π^* is the control policy actually input to the robot, π_{sts} is for the STS motion, and π_{other} is a policy that simply generates gravity compensation torque for supporting the thigh part of the exoskeleton robot.

In order to derive the assist policy π_{sts}, we use the optimal control approach [21], with a physics simulator. To control the exoskeleton robot, one of the methods is to use the joint torques generated when a human performs motions. However, it is not easy to access the actual human joint torque during his/her motion, so a human model approximation is usually required.

In this study, we first build a human approximation model of the user on Multi-Joint dynamics with Contact (MuJoCo) of physics simulator [22] and consider accessing the joint torques by driving the model. In the simulator, since the STS motion is the target of assistance, we applied a triple inverted pendulum model, which was often used in the previous study [21], [23]. We assume that the STS motion is bilaterally symmetrical, and simulate the dynamics of the user's body halved in the sagittal plane. The link parameters of the human model in the MuJoCo were determined with the estimated physical body parameters of each actual subject [24]. Then we calculate the policy to generate STS motion that follows the actual user's trajectory obtained in advance by using iterative linear-quadratic-Gaussian (iLQG) [25]. Here, we have confirmed from our preliminary experiments that the user's natural STS motion varies little from trial to trial, so we assume that the calculated policy can be used in the actual assistive situation. The input state is defined by the joint angle θ and $\dot{\theta}$ as $\mathbf{x} = [\theta_h, \theta_k, \theta_a, \dot{\theta}_h, \dot{\theta}_k, \dot{\theta}_a]^\top$, where the subscripts h, k, and a represent the hip, knee and ankle joint, respectively. The control output $\mathbf{u}$ is the desired joint torques in the simulator: $\mathbf{u} = [\tau_h, \tau_k, \tau_a]^\top$. The optimal policies are obtained by minimizing the value function $v(\cdot)$ as follows:

$$\begin{aligned} v(\mathbf{x},t) &= g(\mathbf{x}(T)) + \sum_{t}^{T-1} l(\mathbf{x},\pi,t) \\ \pi &\leftarrow \arg\min_{\pi} v \end{aligned} \tag{10}$$

where $g(\cdot)$ and $l(\cdot)$ indicate the terminal cost and instantaneous cost, respectively. The terminal cost $g(\cdot)$ for minimization is set as follows:

$$g(\mathbf{x}(T)) = C_{ea}E_a(T) + C_{ev}E_v(T), \tag{11}$$

where $E_a(T) = \|\boldsymbol{\theta}(T) - \boldsymbol{\theta}_{target}(T)\|^2$, $E_v(T) = \|\dot{\boldsymbol{\theta}}(T) - \dot{\boldsymbol{\theta}}_{target}(T)\|^2$, T is the terminal time, $\boldsymbol{\theta}_{target}$ is the target angles, $\dot{\boldsymbol{\theta}}_{target}$ is the target angular velocities at the end of STS motion and $\boldsymbol{\theta}$ represents the hip, knee, and ankle joint angles as $\boldsymbol{\theta} = [\theta_h, \theta_k, \theta_a]^\top$. The instantaneous cost $l(\cdot)$ is set as:

$$\begin{aligned} l(\mathbf{x},\pi,t) &= C_{da}D_a(t) + C_{dv}D_v(t) \\ &\quad + C_u||\mathbf{u}(t)||^2 + C_{ud}||\dot{\mathbf{u}}(t)||^2, \end{aligned} \tag{12}$$

where $D_a(t) = \|\boldsymbol{\theta}(t) - \boldsymbol{\theta}_{target}(t)\|^2$, $D_v(t) = \|\dot{\boldsymbol{\theta}}(t) - \dot{\boldsymbol{\theta}}_{target}(t)\|^2$, and $C_{ea}, C_{ev}, C_{da}, C_{dv}, C_u, C_{ud}$ were manually selected as in most optimal control studies. In this study, we used a fully actuated model in our optimization process as presented in Eq. (10)-(12) with the penalty term for large joint torque output. In the real experiment phase, we assumed that the human subject takes care of the under-actuation problem.

By using the iLQG method, the control law can be acquired as follows:

$$\pi_{sts} = \mathbf{u}^*(t) + L(t)\Delta\mathbf{x}(t), \tag{13}$$

where $\Delta\mathbf{x}(t) = \mathbf{x}(t) - \mathbf{x}^*(t)$ and $L(t)$ is time-dependent local feedback gain. $\mathbf{x}^*(t)$ and $\mathbf{u}^*$ are the optimized open-loop state and the control output of the derived optimal controller, respectively. The optimal knee torque for each subject is shown in Fig. 3(b). In the real knee assistive experiment, the control law related to the knee joint is used as the actual policy π_{sts} by the calculation assuming that the hip and ankle joints follow the optimized state when the user performs the STS motion.

On the other hand, the torque to generate gravity compensation for the thigh robot unit in the sitting situation is used for the π_{other} assuming that the user's feet are in contact with the ground and the leg part is vertical to the ground:

$$\pi_{other} = m_{tr}gl_g\cos\left(\theta_k(t) - \theta_{min}\right) \tag{14}$$

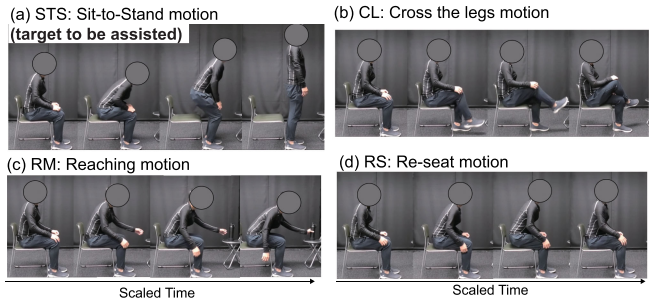

Fig. 4. Candidate motion patterns.

where m_{tr} is the mass of the thigh robot unit, g is the gravity acceleration and l_g is the length from the knee joint to the center of the mass of the thigh link. When the user is in the sitting state, the robot only cancels its weight of the thigh part unit. In addition, the torque generated by the π_{other} hardly interferes with the user's motion other than STS because it's much smaller than the torque to support the human thigh.

The derived final control policy by the estimated user's intention is used both for the right and left exoskeleton robot.

IV. Experimental Setup

A. Motion Tasks

Fig. 4 shows the motion patterns to be verified in this experiment. Fig. 4(a) shows the sit-to-stand (STS) motion to be assisted. In this study, we also verify behaviors that are likely to occur other than the standing-up motion while sitting as shown in Fig. 4(b), (c), and (d), respectively: Cross his legs motion (CL), Reaching motion (RM) and Re-seat motion (RS). In each motion, the subjects were instructed to do as usual, but for the CL motion, they were instructed to raise their right foot. We conducted the experiments with five healthy male subjects (age: 29-58), after obtaining informed consent from them. The human research ethics committee of RIKEN approved the experiment.

B. Positive and Unlabeled Data for PU-Learning

In this study, we measured STS motion for three trials and labeled from initiation of the standing-up to standing state as positive for each trial. This labeling was done manually by carefully observing the joint angles and trunk velocity. On the other hand, we measured two trials for unlabeled data including STS, CL, RM, and RM motions. We asked the subjects to conduct the motions while wearing the exoskeleton robot without the control and collected data by using EMG, gyro sensor, and the robot's angle sensor. We then train the classifier by using the positively labeled data from initiation of the standing-up to standing state for three trials of STS motion and unlabeled data for other motions including STS for two trials. In the actual assistive experiment, the trained classifier was used. Here, the training is conducted for each subject to build the personalized classifier. Since the classifier is applied to sensor data observed in each time step (4 ms), it responds instantly. In the PU-learning, we used logistic regression for the learning method.

C. Feature Extraction

In order to estimate user's motion intention, the processed EMG signals: e, the hip and knee angles: θ_h and θ_k, and the trunk velocity: $\dot{\theta}_{tr}$, were used as the features: $\mathbf{z}'(t) = [e^1(t), e^2(t), e^3(t), e^4(t), \theta_h(t), \theta_k(t), \dot{\theta}_{tr}(t)]^\top$. The ith processed EMG signals e^i are normalized as follows: $e^i(t) = \frac{\varepsilon^i(t) - \varepsilon^i_{rest}}{\varepsilon^i_{mvc}}$, where the EMG signal ε^i is derived as a full-wave rectified and low-pass filtered value of ith raw EMG signals. Here, ε^i_{rest} indicates the resting value and ε^i_{mvc} denotes the maximum voluntary contraction (MVC) output. We obtained these values from the participants in advance of the actual experiment. The EMG signals were measured from right lower limbs with four sensor channels: rectus femoris (e^1), biceps femoris (e^2), lateral head of the gastrocnemius (e^3), and the tibialis anterior (e^4). We used Ag/AgCl bipolar surface EMG electrodes. Using the potentiometers of the right exoskeleton robot system and gyro sensor attached to the user's trunk, we simultaneously obtained the angles of the hip and knee, and the velocity of the trunk. Since most setting motions are bilaterally symmetrical and CL motion also raises the right leg, we used the sensor information about the right leg.

To classify the user's state, we normalized each component of the feature as: $\mathbf{z}(t) = (\mathbf{z}'(t) - \mathbf{Z}'_{\min}) \oslash (\mathbf{Z}'_{\max} - \mathbf{Z}'_{\min})$, where the elements of the vector $\mathbf{Z}'_{\min}$ and $\mathbf{Z}'_{\max}$ are the minimum and maximum of each component of the feature, respectively. These vectors were detected from all of the training data-set. Here, the notation $\oslash$ denotes element-wise (Hadamard) division.

D. Evaluation of the Proposed Approach

In order to evaluate the estimation performance of our proposed approach (after that, *P-AU*), we compared it with standard approaches. Concretely, we considered the following two baseline methods:

1) *STS-PN:* A classifier trained with dataset labeled as negative for sitting and positive for standing-up in STS motion for three trials
2) *P-AN:* All unlabeled datasets are considered negative, and a classifier is trained with a positive and negative dataset.

Both of the above baseline methods also used logistic regression as the learning method. The threshold for discriminating labels from the probabilities was set to 0.5, which is natural for all methods.

The conventional studies on standing up motion assist have focused only on the transition from sitting (negative label) to standing-up (positive label) and assumed a situation in which the state transitions occur only between them. Therefore, they often controlled the robot based on the triggers for the transition from sitting to standing up [9], [10]. The *STS-PN*, which determines the trigger by data-driven, assumes the same transition, and we consider it as the conventional approach. On the other hand, we assume a realistic situation where only part of the selected data are positively labeled and other data including target and non-target motions are unlabeled. In such a situation, it is conceivable to treat unlabeled data as negative. We regarded this situation as *P-AN*. As far as we know, it is also the first study to show what happens to a robot's behavior in the case of *P-AN*.

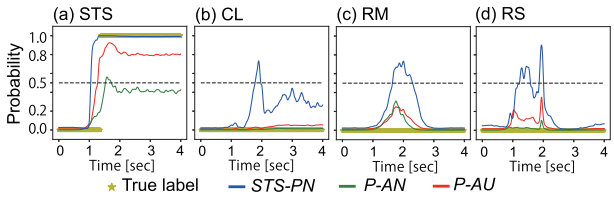

Fig. 5. Probability output from each method. (a) STS. (b) CL. (c) RM. (d) RS. Yellow line shows the actual labels of the standing-up motion state. Blue line shows the probabilities from *STS-PN*. Green line shows the probabilities from *P-AN*. Red line shows the probabilities from *P-AU*. Black dashed line shows probability of 0.5.

TABLE I
CLASSIFICATION EVALUATION

	STS-PN	*P-AN*	***P-AU***
Accuracy	0.913	0.899	**0.995**
F-measure	0.795	0.46	**0.983**

Bold entities indicates our proposed method.

V. RESULTS

In this section, we first represent the motion intention performance when each motion (STS, CL, RM, RS) is performed ten times without driving the exoskeleton robot with representative one subject's data. We then show the performance of five subjects when the exoskeleton robot is driven by adapting each method. In this robot-driven experiment, each motion was performed ten times for three methods (*STS-PN, P-AN, P-AU*).

A. Motion Intention Estimation

Fig. 5 shows the results of the probabilities output from logistic regression for one of ten trials in each method with representative one subject's data. Fig. 5(a) shows results with STS motion, (b), (c) and (d) show CL, RM, and RS, respectively. From Fig. 5(a), the *STS-PN* and *P-AU* methods showed high probabilities in the vicinity of the point when the label became positive, and the *P-AN* method showed a lower value than both. On the other hand, from Figs. 5(b) to (d), although the labels were not positive, the *STS-PN* showed high probabilities when the motions were started, and the *P-AN* and *P-AU* methods showed lower probabilities.

Table I shows the classification accuracy and F-measure which shows the harmonic mean of the recall and the precision when each method is applied to all-time series data for a total of 40 trials (4 motion patterns $\times$ 10 trials). The labels are classified with the threshold set to 0.5 in all methods. Here, in order to calculate each percentage, we consider the standing up motion state as positive and other states as non-positive, and we used data for which all true labels are known. This result indicates that the *P-AU* can estimate the intention with higher performance than the *STS-PN* and *P-AN*.

The learning time was 0.77 seconds on a PC equipped with Intel(R) Xeon(R) CPU E5-1650 v4 at 3.6 GHz. This result indicates that we can apply our approach realistically.

B. Exoskeleton Robot Control Performance

In our online exoskeleton robot control experiment, as shown in equation (9), the robot was driven by the control policies according to the output of the estimated label. However, for safety, we set the final control policy so that once it is switched to π_{sts}, it does not switch until the motion is completed.

TABLE II
PERCENTAGE OF SWITCHING TO STS ASSISTIVE STRATEGIES

Subject	motion type	*STS-PN*	*P-AN*	***P-AU***
A	STS	100	50	100
	Others	97	0	20
B	STS	100	20	100
	Others	67	20	10
C	STS	100	30	100
	Others	70	0	3
D	STS	100	60	100
	Others	67	10	40
E	STS	100	10	100
	Others	100	0	10

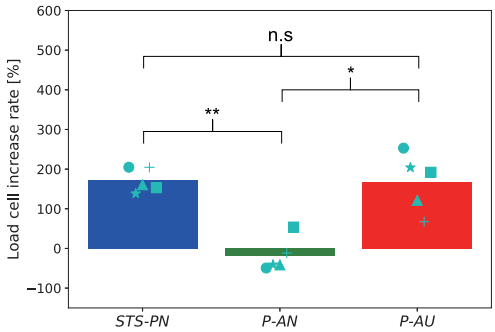

Fig. 6. Comparison between increase rate of load cell from reference value for all methods. Measured load cell value is averaged over time and reference is a time average when the robot alone is driven by the π_{sts}. Symbols show each subject's average for 10 trials of STS motion and bar shows average of all five subjects.

Table II shows the percentage of switching to π_{sts} in all trials for each subject. In the STS motion, the percentage of each method was calculated by dividing the number of switched trials by 10 trials, and in other motions, the percentage was calculated in the same way, but it is the switched ratio in 30 trials (CL $\times$10, RM $\times$10, RS $\times$10). The ideal percentage of STS motion is 100, and that of other motions is 0. From this table, the *STS-PN* and *P-AU* were surely switched, but the *P-AN* was switched only at a low rate in STS motion. In other motions, *STS-PN* switched the policy with high ratios, while *P-AN* and *P-AU* did it with low. These results indicate that the *STS-PN* has a high rate of switching regardless of the motion performed by the user, while the *P-AN* has a low rate regardless of the performed motions. On the other hand, the *P-AU* shows that the policy is switched appropriately according to the motions compared to the baseline methods.

To evaluate the assist of the exoskeleton robot against the users in STS motion for each method, we show the increased rate of the load cell from the reference value in Fig. 6. In this figure, the symbols show the average of ten trials for each subject and the bar shows the average of all subjects. The reference value is a time average when the robot alone without being attached to the user is driven by the STS policy π_{sts}. In this figure, the *STS-PN* and *P-AU* show values exceeding 100, and the *P-AN* shows small. We applied the paired *t*-test adjusted by Bonferroni correction to the three methods. We found significant differences between the *STS-PN* and *P-AN*, and between the *P-AN* and *P-AU* although no-significant difference was found between the

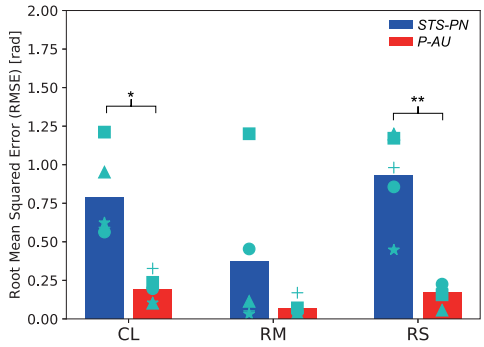

Fig. 7. Exoskeleton control performances of *STS-PN* and *P-AU* in each motion pattern. Joint angle error of each motion pattern is calculated with the averaged trajectories over two trials measured when user performed each motion without any inhibition as the unlabeled data. Symbols show each subject's average for 10 trials of other motions and bar shows average of all five subjects.

STS-PN and *P-AU*. This can be considered that both the *STS-PN* and *P-AU* methods appropriately switched the policy and applied force as the assist from the robot to the user. On the other hand, there are two possible causes for the *P-AN* to show the small value. First, in the trials that the policy did not switch, the user lifted the robot and the load cell did not respond. Second, even in the switched trial, the load cell hardly responded because the timing of switching was late and the user acted first. From these results, we found that the *STS-PN* and *P-AU* were able to appropriately switch the policies to assist the user in the STS motion.

Next, we evaluated the case where the policy was switched in other motions: CL, RM, and RS. From Table II, *P-AN* was excluded from the evaluation because it hardly switched the policy. The fact that the policy did not switch in other motions means that the exoskeleton robot did not interfere with the user's movements. Fig. 7 shows the average of root mean squared error (RMSE) of joint angle in *STS-PN* and *P-AU* for each motion pattern. The symbols show the average of ten trials for each subject and the bar shows the average of all subjects. The joint angle error of each motion pattern is calculated from the averaged trajectories over two trials measured when the user performed each motion without any inhibition as the unlabeled data. We also applied the paired t-test to the RMSE of each motion pattern and found significant differences except for RM motion. The large errors in *STS-PN* are caused by interfering with the user's original intended motion with great force of the exoskeleton robot generated by the π_{sts} which is unsuitable for the other motions (see multimedia attachment). On the other hand, the rate of switching in the *P-AU* method was low, and the robot did not interfere with the user's movement, so the errors were smaller. In the RM motions, the error of *STS-PN* was smaller than other motions. This is because the policy did not switch in the three subjects. From these results, it is clearly shown that our proposed approach is effective using the newly developed lightweight exoskeleton robot.

VI. Conclusions

The previous study [26] suggested a method to properly set the control law generated by the simulation using LQR in consideration of the uncertainty of the parameter when implementing it in the actual sit-to-stand motion. However, the LQR can only be applied within the motion that can be explained linearly. On the other hand, we proposed a method to select the control rule designed by iLQG which can deal with the nonlinear dynamics based on the user's motion intention. Therefore, the dynamics that can be handled and purpose are different from the above paper dealing with things like modeling error.

In this study, we verified the sit-to-stand motion using the robot that can assist limited joints. To increase the target motion to be assisted, we will increase the degree of freedom for the robot and take the method of combining control policies [27] into account in our future studies. In addition, application to weakened people is an important topic. In our future study, we will investigate the adaptation of our method and system to them. Also, we considered a smooth PAM model at this time. Further identifying non-smooth physical terms like Coulombic friction would be beneficial to improve the PAM pressure to force conversion model.

In our selective assist strategy, our current idea is not to use an active assist strategy, e.g., set the target toque to zero, during the transition phase by taking advantage of the lightweight property of our exoskeleton robot.

Acknowledgment

We thank Prof. Kazuaki Kondo and Mr. Takahide Ito for their helpful discussion, and Mr. Akihide Inano for supporting the system development.

References

[1] M. Juszczak, E. Gallo, and T. Bushnik, "Examining the effects of a powered exoskeleton on quality of life and secondary impairments in people living with spinal cord injury," *Topics Spinal Cord Inj. Rehabil.*, vol. 24, no. 4, pp. 336–342, 2018.

[2] K. Gui, H. Liu, and D. Zhang, "A generalized framework to achieve coordinated admittance control for multi-joint lower limb robotic exoskeleton," in *Proc. Int. Conf. Rehabil. Robot.*, 2017, pp. 228–233.

[3] T. Gurriet *et al.*, "Towards restoring locomotion for paraplegics: Realizing dynamically stable walking on exoskeletons," in *Proc. IEEE Int. Conf. Robot. Automat.*, 2018, pp. 2804–2811.

[4] M. K. Shepherd and E. J. Rouse, "Design and validation of a torque-controllable knee exoskeleton for sit-to-stand assistance," *IEEE/ASME Trans. Mechatronics*, vol. 22, no. 4, pp. 1695–1704, Aug. 2017.

[5] A. Kapsalyamov, P. K. Jamwal, S. Hussain, and M. H. Ghayesh, "State of the art lower limb robotic exoskeletons for elderly assistance," *IEEE Access*, vol. 7, pp. 95075–95086, 2019.

[6] M. Rana and V. Mittal, "Wearable sensors for real-time kinematics analysis in sports: A review," *IEEE Sensors J.*, vol. 21, no. 2, pp. 1187–1207, Jan. 2021.

[7] C. Elkan and K. Noto, "Learning classifiers from only positive and unlabeled data," in *Proc. Int. Conf. Knowl. Discov. Data Mining*, 2008, pp. 213–220.

[8] M. A. Alouane, W. Huo, H. Rifai, Y. Amirat, and S. Mohammed, "Hybrid fes-exoskeleton controller to assist sit-to-stand movement," *IFAC-PapersOnLine*, vol. 51, no. 34, pp. 296–301, 2019.

[9] M. E. Mungai and J. W. Grizzle, "Feedback control design for robust comfortable sit-to-stand motions of 3D lower-limb exoskeletons," *IEEE Access*, vol. 9, pp. 122–161, 2021.

[10] V. Rajasekaran, M. Vinagre, and J. Aranda, "Event-based control for sit-to-stand transition using a wearable exoskeleton," in *Proc. Int. Conf. Rehabil. Robot.*, 2017, pp. 400–405.

[11] Q. She, Z. Luo, M. Meng, and P. Xu, "Multiple kernel learning SVM-based EMG pattern classification for lower limb control," in *Proc. 11th Int. Conf. Control Automat. Robot. Vis.*, 2010, pp. 2109–2113.

[12] F. Bian, R. Li, and P. Liang, "SVM based simultaneous hand movements classification using sEMG signals," in *Proc. IEEE Int. Conf. Mechatronics Automat.*, 2017, pp. 427–432.
[13] G. Purushothaman and R. Vikas, "Identification of a feature selection based pattern recognition scheme for finger movement recognition from multichannel EMG signals," *Australas. Phys. Eng. Sci. Med.*, vol. 41, no. 2, pp. 549–559, Jun. 2018.
[14] Y. Yu, X. Sheng, W. Guo, and X. Zhu, "Attenuating the impact of limb position on surface EMG pattern recognition using a mixed-LDA classifier," in *Proc. IEEE Int. Conf. Robot. Biomimetics*, 2017, pp. 1497–1502.
[15] E. Campbell, A. Phinyomark, and E. Scheme, "Linear discriminant analysis with Bayesian risk parameters for myoelectric control," in *Proc. IEEE Glob. Conf. Signal Inf. Process.*, 2019, pp. 1–5.
[16] FESTO, Accessed: Feb. 2022. [Online]. Available: http://www.festo.com
[17] J. Furukawa, T. Noda, T. Teramae, and J. Morimoto, "Human movement modeling to detect biosignal sensor failures for myoelectric assistive robot control," *IEEE Trans. Robot.*, vol. 33, no. 4, pp. 846–857, Aug. 2017.
[18] T. Noda, T. Teramae, B. Ugurlu, and J. Morimoto, "Development of an upper limb exoskeleton powered via pneumatic electric hybrid actuators with bowden cable," in *Proc. IEEE/RSJ Int. Conf. Intell. Robots Syst.*, 2014, pp. 3573–3578.
[19] T. Teramae, T. Noda, and J. Morimoto, "Optimal control approach for pneumatic artificial muscle with using pressure-force conversion model," in *Proc. IEEE Int. Conf. Robot. Automat.*, 2014, pp. 4792–4797.
[20] J. Bekker and J. Davis, "Learning from positive and unlabeled data: A survey," *Mach. Learn.*, vol. 109, pp. 719–760, 2020.
[21] M. Geravand, P. Z. Korondi, and A. Peer, "Human sit-to-stand transfer modeling for optimal control of assistive robots," in *Proc. 5th IEEE RAS/EMBS Int. Conf. Biomed. Robot. Biomechatronics*, 2014, pp. 670–676..
[22] E. Todorov, T. Erez, and Y. Tassa, "Mujoco: A physics engine for model-based control," in *Proc. IEEE/RSJ Int. Conf. Intell. Robots Syst.*, 2012, pp. 5026–5033.
[23] K. Iqbal and A. Roy, "Stabilizing PID controllers for a single-link biomechanical model with position, velocity, and force feedback," *ASME Trans. Biomechanical Eng.*, vol. 126, pp. 838–843, 2004.
[24] D. A. Winter, *Biomechanics and Motor Control of Human Movement*. 4th ed., Hoboken, NJ, USA: Wiley, 2009.
[25] E. Todorov and W. Li, "A generalized iterative LQG method for locally-optimal feedback control of constrained nonlinear stochastic systems," in *Proc. Amer. Control Conf.*, 2005, vol. 1, pp. 300–306.
[26] O. Narvaez Aroche, P.-J. Meyer, S. Tu, A. Packard, and M. Arcak, "Robust control of the sit-to-stand movement for a powered lower limb orthosis," *IEEE Trans. Control Syst. Technol.*, vol. 28, no. 6, pp. 2390–2403, Nov. 2020.
[27] J. Furukawa and J. Morimoto, "Composing an assistive control strategy based on linear bellman combination from estimated user's motor goal," *IEEE Robot. Automat. Lett.*, vol. 6, no. 2, pp. 1051–1058, Apr. 2021.